

Why normal nanosprings do not exist?

Alexandre F. da Fonseca^{1,*}, C. P. Malta^{1,†} and Douglas S. Galvão^{2‡}

¹ *Instituto de Física da Universidade de São Paulo, USP*

Rua do Matão Travessa R 187, CEP 05508-900, São Paulo, SP, Brazil and

² *Instituto de Física ‘Gleb Wataghin’, Universidade Estadual*

de Campinas, Unicamp 13083-970, Campinas, SP, Brazil

Abstract

Helical structures formed from asymmetric rods are classified as *normal* or *binormal* helices, according to the orientation of the rod cross-section. So far, *normal nanosprings* have not been experimentally observed. Here, we provide an explanation for the non-existence of *normal nanosprings* of amorphous material. We show how *binormal nanosprings* can grow from asymmetric catalysts. Our work is based on the vapor-liquid-solid (VLS) growth model of nanosprings [Appl. Phys. Lett. **79**, 1540 (2001)], and on the results obtained by Da Fonseca and Galvão [Phys. Rev. Lett. **92**, 175502 (2004)]. We also explain why a crystalline zinc oxide (ZnO) nanospring cannot be a *normal helix*.

PACS numbers: 81.07.-b, 62.25.+g, 81.16.Hc, 61.46.+w

One of the most important challenges in Nanoscience is the complete understanding of the growing processes of nanostructures. Different types of nanostructures require different methods and processes to produce them. Several groups are working on the development and improvement of these processes motivated not only by the new physical phenomena but also by the great variety of technological applications [1, 2, 3, 4, 5, 6, 7].

In particular, the existence of helically shaped nanowires is of great interest because of the potential applications in nanoelectronics, nanomechanics and nanoelectromechanical systems [8]. Examples of such structures are quasi-nanosprings [9], helical crystalline nanowires [10, 11, 12] and amorphous nanosprings [13, 14, 15].

In contrast to the formation of straight nanowires, the synthesis of helical nanostructures requires either the existence of anisotropy at some level of the growing process or the existence of external forces holding the nanowire in a helical shape. Both cases have been reported in the literature. In the case of amorphous nanosprings, McIlroy *et al* [8, 13] have shown, based on the vapor-liquid-solid (VLS) growth model [16], that the anisotropy in the contact angle between the catalyst and the nanowire induces the helical growth. In the case of crystalline nanosprings, Kong and Wang [12] reported the formation of nanohelices of zinc oxide (ZnO) and showed that the electrostatic interaction between the nanowire and the substrate where it is grown, holds the ZnO nanowires in a helical shape.

Figure 1 displays some examples of amorphous and crystalline nanosprings of different materials (reprinted from [12, 13, 14, 15]). In this Letter, we analyse the helical shape of the nanostructures displayed in Fig. 1 using the modified VLS growth model [8, 13], and the helical structure stability analysis [17, 18] to explain the absence of *normal nanosprings*. We shall introduce the definition of a helical space curve and the basic characteristics of the two possible types of helical structures of a filament with asymmetric cross-section: *normal* and *binormal* helices. In the case of amorphous nanosprings, we use the modified VLS growth model, proposed by McIlroy *et al* [8, 13], to explain the growing process of *binormal nanosprings* showing that the shape of the metallic catalyst must be asymmetric in order to drive the growth of an asymmetric helical nanowire.

A helical space curve is *a curve of constant slope*, *i. e.*, a curve whose tangent lines make a constant angle with a fixed direction in the space (the helical axis) [19]. $\{\mathbf{n}, \mathbf{b}, \mathbf{t}\}$ is a frame, called *Frenet basis*, which is a right-handed orthonormal basis defined at each point along a space curve, where \mathbf{t} is the tangent unit vector, \mathbf{n} is the *normal* unit vector and \mathbf{b}

is the *binormal* unit vector. The plane formed by three points P_1 , P_2 and P_3 belonging to the space curve, where P_2 and P_3 approach P_1 , is called the *osculating plane* of the curve at P_1 [19]. The tangent vector \mathbf{t} belongs to the osculating plane. \mathbf{n} is defined as the unit vector perpendicular to \mathbf{t} , that lies in the osculating plane while \mathbf{b} is defined as the unit vector perpendicular to \mathbf{t} , that is perpendicular to the osculating plane.

Given a rod with asymmetric cross-section, we define the unit vector \mathbf{d} lying in the cross-section plane along the direction of the lowest bending stiffness (it is the direction of the greatest semiaxis for an elliptic cross-section). The helical structure is said to be *normal* (*binormal*) if \mathbf{d} is in the direction of the unit vector \mathbf{n} (\mathbf{b}). In the case of a rod with symmetric cross-section, the *normal* and *binormal* structures degenerate into one type of helix that will be called a *neutral helix*. Figure 2 displays an example of a *neutral*, a *normal* and a *binormal* helix.

An examination of the transmission electron microscopy (TEM) images of the amorphous nanosprings reported in Refs. [8, 13, 14, 15], and in the scanning electron microscopy (SEM) images of the crystalline nanosprings of ZnO reported in Ref. [12], shows that all of them are *neutral* or *binormal* helices and none looks like a *normal* helix (Fig. 2b)). Fig. 1 reproduces some of these nanosprings in order to facilitate the analysis.

The silicon carbide (SiC) nanospring depicted in the bottom right corner of Fig. 1, can be identified as a neutral helix. According to Ref. [15], this nanospring is formed from a nanowire with circular cross-section. The TEM image of a boron carbide nanospring depicted in panel b) of Figure 10 of Ref. [8] (not reproduced here) is also a neutral helix formed from a nanowire of circular cross-section.

The silicon oxide (SiO_2), the boron carbide (BC) and the zinc oxide (ZnO) nanosprings depicted in the bottom left, top left and top right corners of Fig. 1, respectively, are clearly examples of binormal helices. According to Ref. [14], the SiO_2 nanospring is formed from non-cylindrical nanowire. The nanospring depicted in the top left corner of Fig. 1 is formed from a nanowire with rectangular cross-section [8]. The amorphous SiC nanospring reported in Ref. [8] is a binormal helix formed by a nanowire of rectangular cross-section (Figure 13 of Ref. [8] not reproduced here). The ZnO nanohelices reported in Ref. [12] are clearly binormal helices and they are formed from flat nanobelts of rectangular cross-section.

Two questions arise from these experimental observations. 1) *Why normal nanohelices do not exist?* and 2) *how to explain the growing process of a binormal nanohelix?* The

answers to these questions depend on the growing process and on the mechanical properties of the nanospring. We first analyse the case of amorphous nanosprings and then the case of crystalline zinc oxide nanohelices.

The question 1) is interesting because amorphous nanosprings grown by the VLS mechanism are dynamically stable [17], independently of the helical structure being *normal* or *binormal*. According to our previous analysis [17] this stability stems from the intrinsic curvature produced by the catalytic particle in the forming nanospring. The *intrinsic curvature* of a rod represents its tridimensional shape when it is free from external stresses. Goriely and Shipman have studied the dynamical stability of *normal* and *binormal* helices [18] and concluded that intrinsically *normal* or *binormal* helical filaments are always stable. Therefore, from the mechanical point of view, and in agreement with our previous analysis [17], both types of helical amorphous nanostructures can occur.

In order to answer the questions 1) and 2) for amorphous nanosprings, we assume that the metallic catalyst have asymmetric shape, and the modified VLS growth model is used to explain the absence of *normal nanosprings*. The growing process of a *binormal nanospring* is also explained by the modified VLS growth model.

Following the VLS growth model, a liquid droplet of a metal absorbs the material from the surrounding vapor and after super-saturation of the absorbed material within the droplet, the excess material precipitates at the liquid-solid interface forming the nanowire beneath the metallic catalyst. The model is based on the interaction between the surface tension of the liquid-vapor (γ_{LV}), solid-vapor (γ_{SV}) and solid-liquid (γ_{SL}) interfaces. McIlroy *et al* [8, 13] proposed that the helical growth process occurs due to a contact angle anisotropy (CAA) at the catalyst-nanowire interface. The trajectory of the metallic catalyst is driven by the work needed to shear it from the surface of the nanowire. This work is called the thermodynamic work of adhesion W_A and can be computed in terms of the surface tensions by [8]:

$$\begin{aligned} W_A &= \gamma_{SV} + \gamma_{SL} - \gamma_{LV} \\ &= \gamma_{SV}(1 - \cos \theta) \end{aligned} \tag{1}$$

where θ is the angle between the surface tensions γ_{SL} and γ_{SV} . Figure 3a) reproduces the schematic diagram of a spherical catalyst located asymmetrically on the nanowire, in accordance to the modified VLS growth model [8].

Spherical catalysts, by symmetry, produce helical nanowires with circular cross-section. In order to produce a helical nanowire with asymmetric cross-section, as the amorphous nanosprings displayed in top and bottom left corners of Fig. 1, we propose that the metallic catalyst must be asymmetric so as to induce the growth of helical nanowires with asymmetric cross-section. The panels b) and c) of Fig. 3 display two schematic diagrams for the growth of *normal* and *binormal* helical nanowire, respectively, with elliptic cross-section. In these schemes, the elliptical metallic catalyst possesses semiaxes B and A with $B > A$.

According to McIlroy *et al* [13], if the diameter of the spherical catalyst increases systematically, the CAA becomes less significant and the work of adhesion returns to that of the symmetric configuration in which the nanowire grows linearly. In terms of the diagram displayed in Fig. 3a), this happens when $\Delta/R \ll 1$.

In the case of an asymmetric catalyst, the magnitude of B (A) will determine the significance of the CAA for the scheme depicted in Fig. 3b) (Fig. 3c)). We expect that the scheme displayed in Fig. 3b) is less favourable to the growth of a helical nanowire because Δ/B is always smaller than Δ/A . Therefore, the growth of a *normal nanospring* is less favoured than the growth of a *binormal nanospring* if $(B - A)$ is large. If $B \simeq A$, the growth of *normal* or *binormal* helices are equally favoured, but the shape of the catalyst is approximately spherical, so the helical structure cannot be easily distinguished from the *neutral* helix.

The explanation for the asymmetric growth of the *binormal nanospring* is the same as that proposed by McIlroy *et al*: the growth rate velocities are larger at the interfaces with small θ [8, 13]. Since the projection of the elliptic catalyst onto a plane perpendicular to the axis of the linear nanowire is a circle of radius A , for the diagram depicted in Fig. 3c), the condition for the optimal geometry to promoting helical growth can be inferred from that obtained by McIlroy *et al* for the growth of a helical nanowire in the case of a spherical catalyst (Fig. 3a)), where the radius of the spherical catalyst must be replaced by A : $A/\rho \simeq 1.5$ [8, 13].

The formation of helical nanowires of rectangular cross-section, as those displayed on the top left corner of Fig. 1, and in Figure 13 of Ref. [8], can be explained using the modified VLS growth model for a rectangular metallic catalyst. If the smallest side of the rectangular catalyst is not larger than the displacement Δ , the CAA is significant and the helical growth can occur.

The stability analysis of helical rods can be used to answer the questions 1) and 2) regarding crystalline *normal nanosprings*. In the case of the growth of ZnO nanohelices

reported by Kong and Wang [12], the growing process is not driven by a catalytic particle. The resulting helical nanostructure does not possess intrinsic curvature [17] and we must resort to stability analysis to obtain the conditions for the existence of helical structure.

Goriely and Shipman [18] have shown that *normal* helical rods, without intrinsic curvature, are unstable, and that only flat finite *binormal* helices, clamped at both ends, can be dynamically stable. This explains why Kong and Wang obtained only *binormal nanosprings*, as the example depicted on the top right corner of Fig. 1. Kong and Wang [12] have shown that the helical shape is maintained by the electrostatic interaction between the spontaneous polarization of the thin crystalline nanobelt, and the substrate where it is grown, thus maintaining the ends of the ZnO nanohelix fixed.

In conclusion, we have studied the helical features of several types of nanosprings reported in the literature. The TEM and SEM images of several nanosprings and nanohelices were analysed and we have verified the non-existence of one type of helical structure: *normal nanohelix*. We have used the modified VLS growth model, and the stability analysis of helical rods, to explain both, the growing process of the nanosprings seen in the TEM and SEM images, and why *normal nanosprings* do not exist.

In the case of amorphous nanosprings, we proposed that the asymmetry in the shape of the metallic catalysts induces the growth of asymmetric helical nanostructures. The anisotropy in the work of adhesion along the interface liquid-solid is less significant in the case of the growth of a *normal nanohelix* than that for the growth of a *binormal nanohelix*.

Therefore, we conclude that there is a relation between the type of the helical nanostructure, the shape of its cross-section and the shape of the metallic catalyst. So, from the type and shape of the nanospring it is possible to infer the shape of the metallic catalyst. For example, if the period of the turns changes along the nanospring, as it is seen in the SiO₂ nanosprings of Ref. [14] (see the bottom left corner of Fig. 1), our analysis suggests that the size and shape of the catalyst has changed during the nanospring formation.

In the case of crystalline nanosprings that do not possess intrinsic curvature, the existence of the *binormal nanohelix* is explained in terms of the stability analysis of helical rods with asymmetric cross-section [18]. We have shown that this analysis completely explains the main characteristics of the formation of zinc oxide (ZnO) *binormal nanosprings*.

Normal and *binormal* helical nanostructures may lead to different technological applications. Our results are in perfect agreement with the experimental TEM and SEM images

of various nanosprings and provide new insight on the geometric and mechanical characteristics of both types of helices. It is well established that for some growing phenomena at nanoscale the presence of the catalytic particles is fundamental, nevertheless the details of how they define the nanostructures morphology is not well understood. In the present work, we show how the catalytic particle shape is important to determine the morphological symmetries. The catalytic particle shape is also responsible for the nonexistence of *normal nanosprings*. We expect that our analysis will stimulate further theoretical and experimental investigations about the growth process of helical nanostructures.

This work was partially supported by the Brazilian agencies FAPESP, CNPq and FINEP.

* afonseca@if.usp.br

† coraci@if.usp.br

‡ galvao@ifi.unicamp.br

- [1] S. Iijima, *Nature (London)* **354**, 56 (1991).
- [2] R. H. Baughman, A. A. Zakhidov and W. A. de Heer, *Science* **297**, 787 (2002).
- [3] L. Samuelson, *Mater. Today* **6** (10), 22 (2003).
- [4] A. S. Edelstein and R. C. Cammarata, *Nanomaterials: synthesis, properties and applications*, Institute of Physics Publishing, Bristol (1996).
- [5] K. W. Wong, X. T. Zhou, F. C. K. Au, H. L. Lai, C. S. See and S. T. See, *Appl. Phys. Lett.* **75**, 2918 (1999).
- [6] M. S. Gudiksen, L. J. Laudon, J. Wang, D. C. Smith and C. M. Lieber, *Nature (London)* **415**, 617 (2002).
- [7] H. I. Liu, D. K. Biegelsen, F. A. Ponce, N. M. Johnson and R. F. W. Pease, *Appl. Phys. Lett.* **64**, 1383 (1994).
- [8] D. N. McIlroy, A. Alkhateeb, D. Zhang, D. E. Aston, A. C. Marcy and M. G. Norton, *J. Phys.: Condens. Matter* **16**, R415 (2004).
- [9] Y. H. Tang, Y. F. Zhang, N. Wang, C. S. Lee, X. D. Han, I. Bello, S. T. Lee, *J. Appl. Phys.* **85**, 7981 (1999).
- [10] H. F. Zhang, C. M. Wang, L. S. Wang, *Nano Lett.* **2**, 941 (2002).
- [11] S. Amelinckx, X. B. Zhang, D. Bernaertsm X. F. Zhang, V. Ivanov and J. B. Nagy, *Science*

265, 635 (1994).

[12] X. Y. Kong and Z. L. Wang, *Nano Lett.* **3** 1625 (2003).

[13] D. N. McIlroy, D. Zhang, Y. Kranov and M. G. Norton, *Appl. Phys. Lett.* **79**, 1540 (2001).

[14] H. F. Zhang, C. M. Wang, E. C. Buck and L. S. Wang, *Nano Lett.* **3**, 577 (2003).

[15] D. Zhang, A. Alkhateeb, H. Han, H. Mahmood, D. N. McIlroy and M. G. Norton, *Nano Lett.* **3**, 983 (2003).

[16] R. S. Wagner and W. C. Ellis, *Appl. Phys. Lett.* **4**, 89 (1964).

[17] A. F. da Fonseca and D. S. Galvão, *Phys. Rev. Lett.* **92**, 175502 (2004).

[18] A. Goriely and P. Shipman, *Phys. Rev. E* **61**, 4508 (2000).

[19] D. J. Struik, *Lectures on Classical Differential Geometry*, 2nd Edition, (Addison-Wesley, Cambridge, 1961).

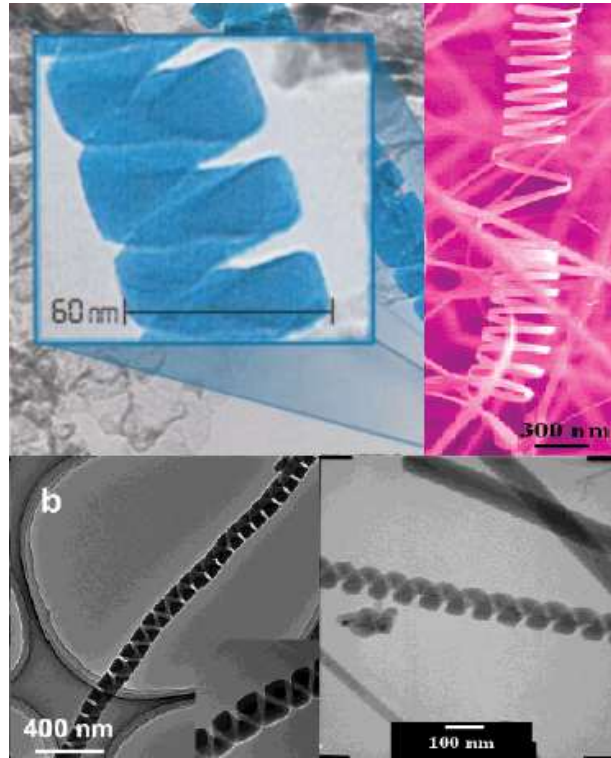


FIG. 1: (Color online) Examples of nanosprings of different materials. Top left corner: amorphous Boron Carbide, BC, [13]; Top right corner: crystalline Zinc Oxide, ZnO [12]; Bottom left corner: amorphous Silicon Oxide, SiO₂, [14]; Bottom right corner: amorphous Silicon Carbide, SiC, [15]. Figures reprinted with permission.

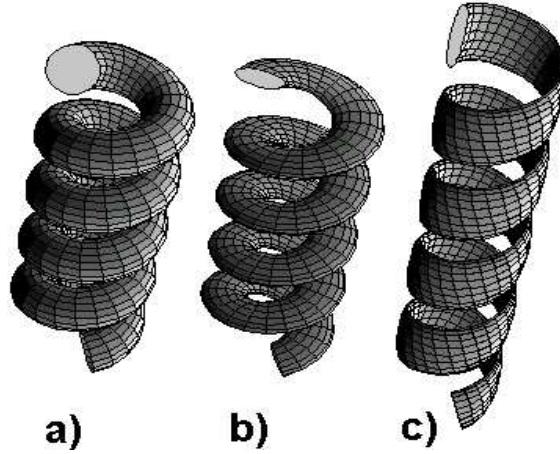


FIG. 2: a) *Neutral* helix made of a rod with circular cross section, b) *normal* and c) *binormal* helices made of a rod with an asymmetric cross-section.

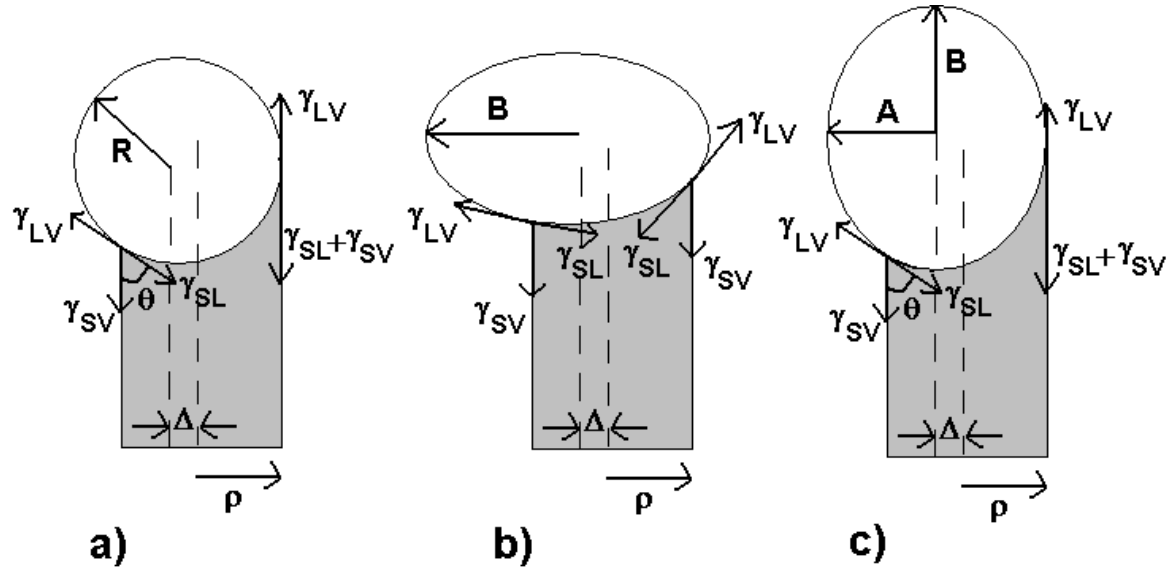


FIG. 3: Schematic diagrams of a) spherical and b) and c) elliptical catalysts whose center is shifted of Δ with respect to the axis of the nanowire. The corresponding surface tensions vary with θ along the interface liquid-solid. ρ is the radius of the nanowire cross-section. R is the radius of the spherical catalyst, and A and B are the smallest and the greatest semiaxes of the elliptical catalyst, respectively.